Experimental Cell Research 347 (2016) 14–23

Contents lists available at ScienceDirect

Experimental Cell Research

journal homepage: www.elsevier.com/locate/yexcr

Research Article

Intracellular insulin quantification by cell-ELISA

Parker Lyng Andersen, Patrick Vermette *

Department of Chemical and Biotechnological Engineering, Université de Sherbrooke, 2500, boul. de l'Université, Sherbrooke, QC, Canada J1K 2R1

ARTICLE INFO

Article history:
Received 26 April 2016
Received in revised form
21 June 2016
Accepted 22 June 2016
Available online 23 June 2016

Keywords:
Intracellular insulin
Cell-ELISA
Cell number
INS-1 cells
Pancreatic islet culture and β-cells
MafA downregulation

ABSTRACT

Current methods of monitoring insulin in culture are limited to soluble insulin (secretions or lysates) or synthetic gene reporter analyses. We present an insulin-specific cell enzyme-linked immunosorbent assay (cell-ELISA) to assess relative intracellular insulin protein content of adherent cultures, normalized to cell density with further immunocytochemical verification of insulin-expressing cells within identical cultures. The protocol was optimized and validated using an insulin-expressing cell line (INS-1) by confirming direct relations between intracellular insulin content and insulin-expressing cell density, in a glucose exposure-dependent manner. Utility was demonstrated by identifying multiple INS-1 clones lowly expressing insulin following lentiviral particle delivery of interference RNA intended to down-regulate one of the insulin gene-directed transcription factors, MafA. The cell-ELISA was also applied to monitor insulin content within partially dissociated primary mouse islet cultures. This technique allows for the first time routine analysis of intracellular insulin protein *in vitro* suitable for investigating islet cell biology by means of multiple parameter screening.

1. Introduction

The endemic prevalence of Diabetes Mellitus continues to increase significantly. Diabetes Mellitus is initiated by various mechanisms and failures, and to simplify involves the loss of circulating glucose restriction due to an inadequacy in insulin signaling. Continued elevated circulating glucose levels are strongly linked to various vasculature problems, metabolic syndrome and several neuropathies with inevitable progressive and often devastating consequences; although sometimes temporarily manageable it is virtually incurable. In most vertebrates, circulating glucose is stringently controlled through its storage and release by various tissues, predominantly under the incentive of hormones derived from the "Islets of Langerhans" located within the pancreas. Within healthy individuals in response to fluctuating glucose levels, islet α-cells release the hormone glucagon promoting glucose mobilization, whereas islet β-cells release the hormone insulin promoting glucose storage, each intended to respectively minimize hypoglycemia or hyperglycemia. Ultimately, Diabetes Mellitus involves the loss of β-cell mass and/or function. Significant developments are progressing with respect to expanding functional islet cell mass *in vitro* and *in vivo* as a scheme to restore insulin requirements [1]. However, fundamental understanding regarding particular aspects of β-cell biology and insulin biochemistry are poorly characterized, primarily due to technical difficulties in routinely characterizing intracellular insulin protein expression and content.

The aim here was to develop a new method of routinely and efficiently monitoring intracellular insulin content of cultured islet cells. Currently, islet and β-cell functionality is most often monitored by insulin release, typically in response to altering glucose, nutrients or other secretagogue exposure. Extracellular assays are potentially problematic because unintentionally induced necrosis will potentially release significant amounts of insulin which will be erroneously interpreted as physiologic secretions. Current methods to analyze intracellular insulin expression requires cumbersome lysate analysis of mRNA, protein (by radio-immunoassays or sandwich-ELISAs) or manufactured gene-reporter analysis. Commercially available assay kits used for both extracellular and lysate insulin protein determination requires significant financial obligations restricting sample number analysis. Our own inability to measure insulin using typical Western blotting techniques from cell lysates (or purified commercial insulin) reflects the lack of published intracellular insulin data. An alternative method of protein quantification is the cell enzyme-linked immunosorbent assay (cell-ELISA), which has been utilized in specific but infrequent applications [2, 3 as examples]. We describe an insulin-specific cell-ELISA procedure which is normalized

Abbreviations: Ab, antibody; ELISA, enzyme-linked immunosorbent assay; HRP, horseradish peroxidase

* Corresponding author.
E-mail addresses: prk.andersen@gmail.com (P.L. Andersen), Patrick.Vermette@USherbrooke.ca (P. Vermette).

http://dx.doi.org/10.1016/j.yexcr.2016.06.014
0014-4827/

to cell density, and confirmed by immunocytochemistry sequentially on identical islet cell cultures. We show that this technique is applicable to efficiently and routinely screening multiple parameters of interest simultaneously for insulin content as a practical alternative to soluble insulin analysis.

2. Results and discussion

2.1. The cell-ELISA technique specifically recognizes insulin in INS-1 cell cultures

The INS-1 cell line, an insulin-expressing rat β-like cell line [4], was utilized to develop and optimize the anti-insulin cell-ELISA

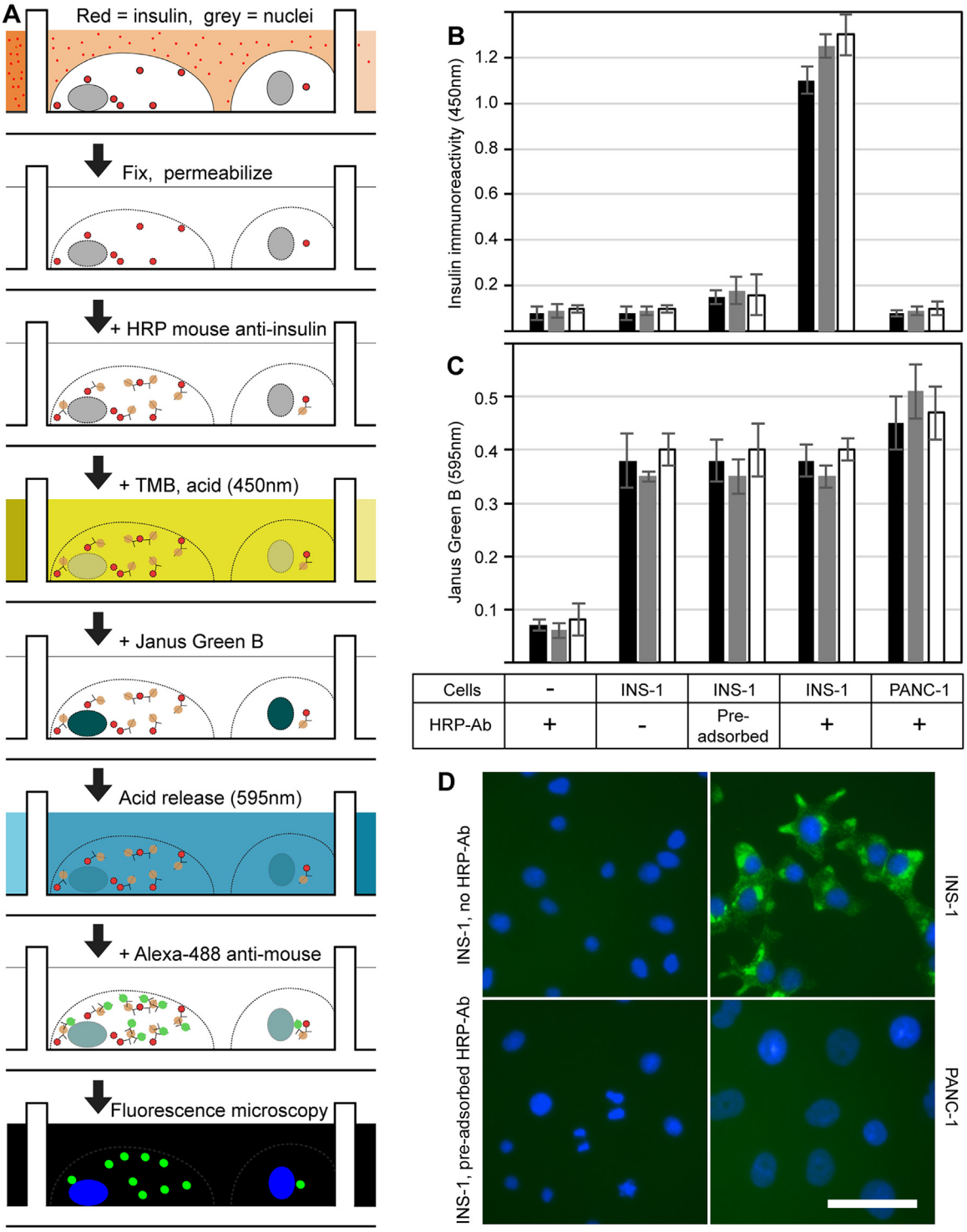

Fig. 1. The cell-ELISA protocol and its verification. Identical cultures are processed in series (A) and quantified by absorbance at 450 nm for insulin (B) and at 595 nm for Janus Green B release (C). Anti-insulin immunocytochemistry (green immunofluorescence with Hoechst 33258 counterstain to identify nuclei) (D) is dependent upon the presence of anti-insulin antibody and INS-1 cells. As negative controls, the antibody was either omitted or pre-adsorbed with excess insulin, or PANC-1 cells were used in place of INS-1 cells. Bars in "B" and "C" represent averages of original unprocessed absorbances of six to eight wells from three independent experiments (black, gray and white). Error bars represent standard deviations. Scale bar in "D" = 50 μm.

technique. A graphic representation of the procedure is given in Fig. 1A. To demonstrate specificity, INS-1 cells were seeded at 4000 cells per well in a 96-well plate and cultured for 3 days. Typically, six to eight wells per condition were assayed. Briefly, in 96-well plates, identical cultures are processed sequentially for insulin immunoreactivity (cell-ELISA, Fig. 1B), cell density (Janus Green B staining and release, Fig. 1C) and insulin immunocytochemistry (fluorescent targeting of the initial antibody applied in the cell-ELISA, Fig. 1D). When desired, prior to cell-ELISA analysis, samples of conditioned media are collected and frozen for further investigation of any particular wells of interest. Periodically throughout the procedure, to characterize morphology of the cultures observations were made by eliminating the meniscus within wells of interest, allowing proper Köhler illumination and phase ring alignment (Supplemental Fig. 1). Culture plates were shaken for 8 s on a titer-plate shaker to remove loose debris before addition of fixative. The fixative was added directly to the existing culture medium gently to minimize cell disruption. Following the first 20 min of fixation, the plates were left shaking nearly continuously throughout the procedures to ensure efficient exposure and uniform reactions of all substrates. Continuous shaking does not alter the cellular content of the procedure (Supplemental Fig. 2) but does remove much of the debris including osmotically lysed cells following intentional replacement of medium with water in selected wells (Supplemental Fig. 3). Following fixation, cultures were permeabilized with Triton X-100 and processed for immunoreactivity using a horseradish peroxidase (HRP)-conjugated anti-insulin antibody (HRP-Ab) which recognizes insulin from multiple species (as per supplier's product data sheet). The term “insulin” used in this report is assumed to include insulin, pro-insulin and intermediate structures, as we have to acknowledge the antibody recognizes all forms (as per supplier's product data sheet). Utilizing commercial TMB ELISA substrate, horseradish peroxidase produces a soluble colored end-product and its absorbance when measured at 450 nm (following acid stabilization) is proportional to bound HRP-Ab. Therefore, absorbance (450 nm) represents insulin content of each culture well. When INS-1 cells were processed for insulin immunoreactivity (HRP-Ab derived), a positive reaction was observed (Fig. 1B). Immunoreactivity was virtually eliminated when the HRP-Ab was previously pre-adsorbed with soluble commercial insulin, and absent in wells containing PANC-1 cells (a human pancreatic ductal, non-islet, non-insulin expressing cell line) in place of INS-1 cells. Additionally, no immunoreactivity was seen in wells void of cells, nor in wells containing INS-1 cells without the presence of HRP-Ab. Combined, this indicates immunoreactivity from HRP-Ab in the cell-ELISA reflects the insulin content of INS-1 cell cultures. All bar graphs in this manuscript depict means $\pm$ standard deviations within each experiment. Triplicates (black, gray and white bars) are included to demonstrate variations between experiments. Data presented as bar graphs therefore represents variances within and between repeated experiments.

Following the initial cell-ELISA procedure, identical wells were then processed to normalize insulin immunoreactivity to cell density by Janus Green B binding and release, which in INS-1 cells following the cell-ELISA procedure was retained predominantly within nuclei until acid-induced release (Supplemental Fig. 4). Under acidic conditions nuclear bound Janus Green B becomes a colored soluble product which was measured by absorbance at 595 nm [5] (Fig. 1C). The acid release step was performed in a 140 mM salt solution in an attempt to preserve the original HRP-Ab/antigen interaction. An increase in absorbance (A595nm) coincided with wells containing intact cells (Fig. 1C). As expected, PANC-1 cells presented no detectable anti-insulin immunoreactivity but did display a Janus Green B reaction. Insulin content and cell density are therefore resolved independently within identical culture wells, and supports the notion that cell-ELISA-derived anti-insulin immunoreactivity is dependent specifically upon insulin containing cells (INS-1 as opposed to PANC-1 cells). Further analysis of the cultures by application of a fluorescently-labeled goat anti-mouse antibody intended to recognize the initially applied HRP-Ab resulted in positive immunofluorescence, which paralleled that of the cell-ELISA immunoreactivity (Fig. 1B and D). Positive anti-insulin immunocytochemistry was observed in INS-1 cells, but absent when the HRP-Ab was omitted or pre-adsorbed with commercial insulin. Anti-insulin immunocytochemistry was also absent in PANC-1 cells. Although anti-insulin immunocytochemistry of INS-1 cells yielded a visually reduced signal intensity following the first two procedures (cell-ELISA and Janus Green B staining), the resulting staining pattern reflected what was expected, matching appearance to that of cultures not processed for cell-ELISA and Janus Green B stain (Supplemental Fig. 5). Additionally, because PANC-1 cells exhibit no anti-insulin immunocytochemistry by either cell-ELISA or immunocytochemistry, it was concluded that an artificial epitope is not being created. Combined, these data indicate that the cell-ELISA specifically recognized insulin within the INS-1 cell cultures. We are unable to demonstrate a similar retention of antigen-Ab complex utilizing an anti-cytokeratin-19 antibody required to identify PANC-1 ductal cells. This suggests not all antigen-antibody complexes are sufficiently stable to sustain the procedure.

To demonstrate sensitivity of the assays, INS-1 and PANC-1 cells were counted using a hemocytometer (in our hands with expected accuracy of no more than $\pm$ 20%), serially diluted two-fold, seeded on poly-L-lysine to maximize plating efficiency, and cultured for 14 h (to minimize proliferation of the INS-1 cells). Cultures were then processed sequentially for insulin immunoreactivity (the cell-ELISA assay) and cell density (the Janus Green B staining assay). Statistical p-values were calculated between averaged optical densities of the cultures initiated at different cell densities. This procedure allows determining the assay sensitivity with respect to the lower detection limit, and to compare cell densities. Details from Supplemental Fig. 6 indicate insulin immunoreactivity can be observed from as low as approximately 300 INS-1 cells seeded per well ($312 \pm 20\%$ in table of Supplemental Fig. 6) with respect to negative control (blank) wells, assuming a requirement of a p-value < 0.005, and non-overlapping standard deviation bars. However, the assay cannot detect a significant difference between 312 and 625 cells under the same criteria. Based on the same above statistical criteria, a similar sensitivity was observed for the cell density when utilizing the Janus Green B assay (Supplemental Fig. 7), providing a lower limit of statistically significant detection of approximately 625 INS-1 cells. However, given the order of magnitude and the narrow range of optical densities obtained for background insulin immunoreactivity from PANC-1 cells, although if p-values may be statistically significant, for practical purposes the lower limit of cell density should not be derived purely on p-values. For this reason, our routine cell-ELISA analyses typically involve seeding between 4000 and 40,000 cells per well such that optical densities result in values between 0.1 and 1.4 (through 200 μL of solution in each assay well of a 96-well culture plate) to consider statistical p-values and standard deviations relevant (Supplemental Figs. 6 and 7). Practically, we consider the lower limit for this technique to be not below 2000 INS-1 cells per well. Although immunoreactivity sensitivity may be increased, such as by increasing antibody incubation time, or utilizing antigen retrieval mechanisms (for examples), the Janus Green B sensitivity is not anticipated to be increased, and therefore attempts were not prioritized to increase sensitivity.

It is important to mention that optical densities between two cell types stained with Janus Green B should not be compared. For

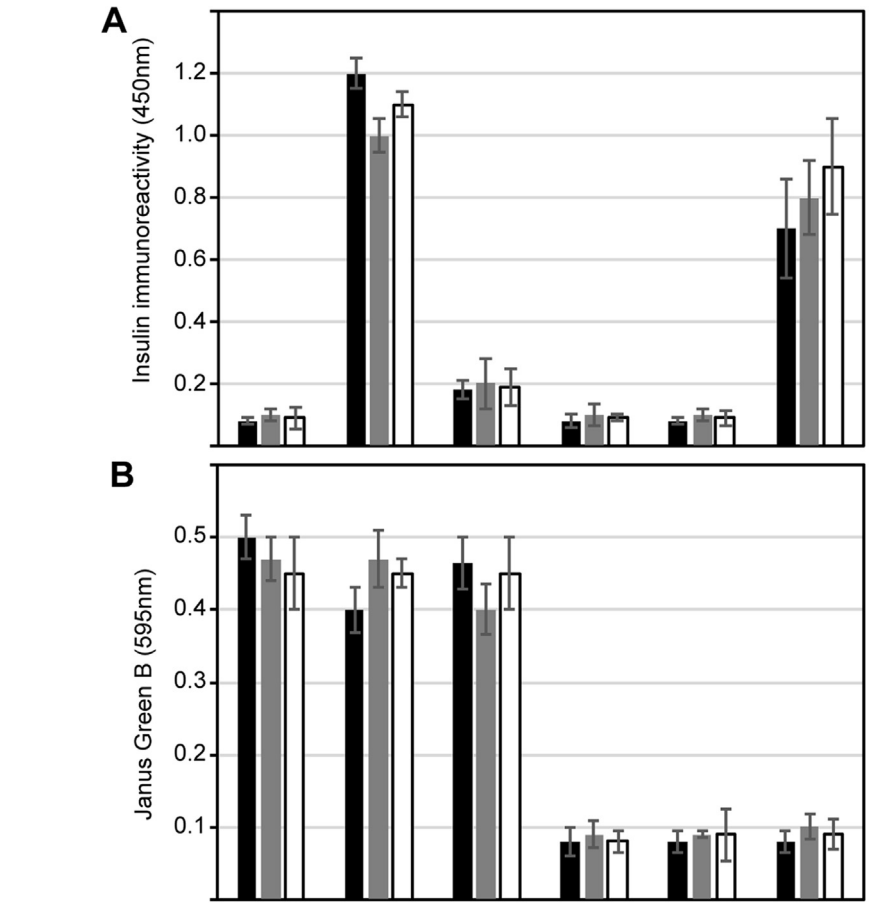

INS-1 cells	+	+	+	Lysed	-	-
HRP-Ab	-	+	+	+	+	+
Permeabilization	+	+	-	+	+	+
Capture antibody	-	-	-	-	-	+
Insulin spike	-	-	-	-	+	+

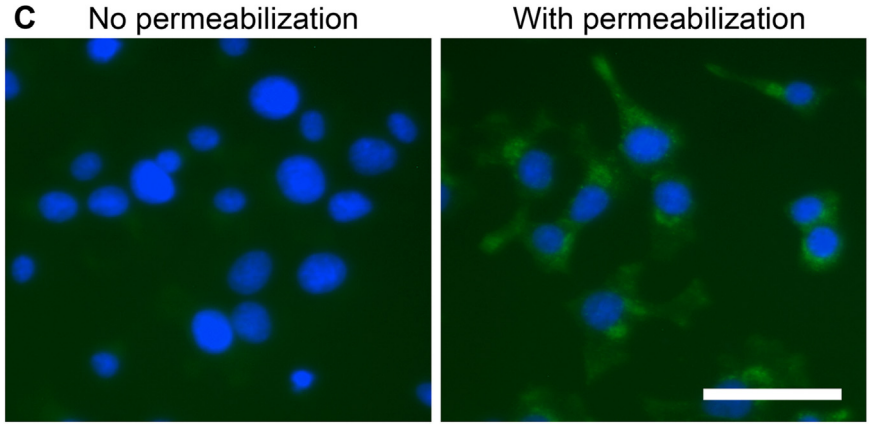

Fig. 2. Anti-insulin immunoreactivity is intracellularly derived. To determine if immunoreactivity was of intracellular origin, INS-1 cells were processed in the absence of HRP-Ab, without permeabilization, and following osmotic lysis for insulin immunoreactivity (A) and Janus Green B staining (B). Fluorescent images with and without permeabilization are presented (C). To determine if exogenous soluble insulin affects immunoreactivity, wells were processed with and without an anti-insulin capture antibody previously attached to the culture plate surface. Bars represent averages of original unprocessed absorbances of six to eight wells from three independent experiments (black, gray and white). Error bars represent standard deviations. Scale bar in "C" = 50 μm.

example, under these conditions, 14 h after seeding, INS-1 cells are in a lag period with little or no mitotic cells observed. Whereas PANC-1 cells were highly proliferating with little or no lag period, and demonstrated an increase in cell density over this culture period. Therefore, significantly higher optical densities were observed with PANC-1 cells when compared to those of INS-1 cells after seeding at approximately the same densities (Supplemental Fig. 7). Additionally, because the mechanism of Janus Green B staining of fixed cells is unknown, particular cell types may exhibit alternative staining profiles. Regardless, a direct linear correlation

between cell density and Janus Green B optical density was repeatedly obtained within a given cell type.

2.2. Anti-insulin cell-ELISA immunoreactivity is intracellularly derived

We next sought to determine if insulin immunoreactivity, as measured by cell-ELISA, reflects intracellular and/or extracellular insulin (Fig. 2). When the permeabilization step (0.5% Triton X-100) was omitted in an attempt to restrict HRP-Ab entry into the cells, anti-insulin immunoreactivity was virtually eliminated (Fig. 2A). Furthermore, when cultures were osmotically lysed by exchanging the culture medium with water, cells burst and were easily washed away during the agitation procedure (Supplemental Fig. 3), which again resulted in no cell-ELISA immunoreactivity (Fig. 2A). This suggests that soluble insulin does not contribute to cell-ELISA immunoreactivity. Additionally, when commercial insulin was spiked into culture medium in the absence of cells one hour before fixation, cell-ELISA immunoreactivity was absent. The lack of immunoreactivity against spiked insulin was reversed after a previous application of a capture antibody (an anti-insulin antibody recognizing a distinct insulin epitope than that recognized by HRP-Ab, often used in sandwich-ELISAs) to the culture plate. This confirmed that the presence of soluble insulin was not detected by cell-ELISA (Fig. 2A). Furthermore, Janus Green B staining confirmed the requirement of intact cells for insulin immunoreactivity (Fig. 2B).

Combined, these data confirm that anti-insulin cell-ELISA recognizes predominately intracellular insulin content and renders the assay distinct from basal-level release or glucose-stimulated insulin secretion experiments which monitors soluble insulin. Small amounts of insulin have been reported on the surface of β-cells during high-glucose stimulation, and attributed to a small portion of fused vesicles (to the plasmalemma) which exocytose partially or slowly [6]. Since we routinely keep INS-1 cells in 5.6 mM (except where mentioned) significant surface insulin was not expected and was not observed. Therefore, lysed cells, secreted insulin and surface insulin are not significantly contributing to immunoreactivity in this system.

2.3. Chronic hyperglycemia suppresses insulin content

We next sought to validate the technique utilizing an experimental manipulation predicted to directly influence insulin content. From the published literature, insulin expression is anticipated to decrease during chronic hyperglycemia, possibly due to downregulation of the transcription factor MafA [7,8]. We hypothesized the anti-insulin cell-ELISA would be appropriate to determine the effects of increased glucose exposure on insulin content. INS-1 cells were cultured at different densities for 5 days in either physiological (5.6 mM) or hyper-physiological glucose (28 mM) concentrations. Plotting cellular insulin immunoreactivity (cell-ELISA, A 450 nm) in function of cell density (Janus Green B, A 595 nm) decisively revealed that 1) insulin content was directly proportional to cell density ($R^2 > 0.99$), but in distinctly different relations depending upon either high- or low-glucose environments; and 2) both insulin content and cell density were affected by glucose concentration (Fig. 3A). Specifically, high-glucose resulted in a greater number of cells present with a concurrent reduction in insulin content. One representative experiment is depicted in Fig. 3, and two additional independent experiments designed identically are shown in Supplemental Fig. 8 to demonstrate experimental variation. No obvious effect on cell viability was observed. Importantly, these data immediately advocate further questions (intentionally not addressed here), such as is the decrease in insulin content following hyperglycemia a function of insulin release and/or a result of cell division diluting cellular insulin granules, as possible alternatives to a reduction in insulin mRNA stability as predicted from the literature [7,8]. The high R^2 values (typically > 0.97) demonstrate linearity over a range of cell densities, further validating the system (Fig. 3A) and demonstrating the effectiveness in normalizing insulin immunoreactivity to cell density (Janus Green B).

To validate these initial observations of reduced insulin, we compared sister cultures in parallel by two different methods. One set of wells was used for insulin immunoreactivity by cell-ELISA (Fig. 3B) alongside another set to monitor insulin content of cell lysates (Fig. 3C). Lysates were prepared using Triton X-100 to disrupt the cells. Triton X-100 lysis, which was previously used

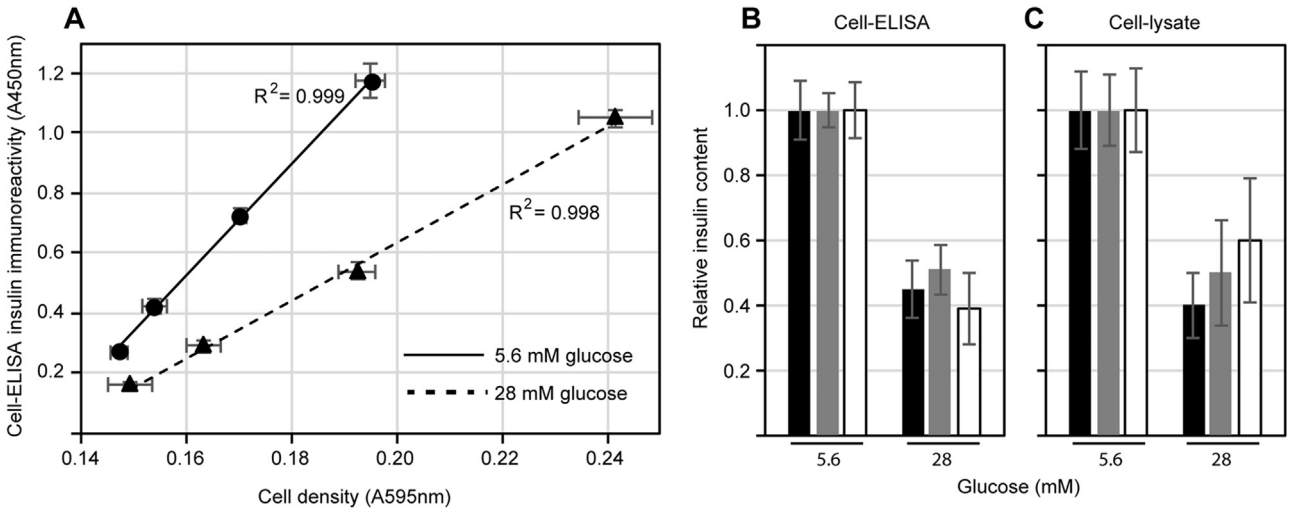

Fig. 3. Validation of the cell-ELISA assay. INS-1 cells were initiated at various densities identically between the two glucose conditions. Insulin immunoreactivity (A 450 nm) and Janus Green B release (A 595 nm) were determined after five-day exposure to 5.6 mM (solid line) or 28 mM (dashed line) glucose (A). Each point represents an average of six wells, error bars represent standard deviations of one representative experiment and R^2 values are included to demonstrate linearity. Additional data to demonstrate variations between experiments are included in Supplemental Fig. 8. To compare cell-ELISA immunoreactivity to lysate analysis, sister wells (seeded with identical numbers of cells) were processed by cell-ELISA (B) or cell-lysate analysis using a commercial assay kit (C) following 5-day exposure to either 5.6 or 28 mM glucose. Data points in (A) represent averages of raw immunoreactivity (original unprocessed absorbance) of six wells. Bars in (B) and (C) represent averages of 4 wells (cell-ELISA) or 3 wells (cell-lysate analysis) normalized to 5.6 mM glucose. Bars in "B" and "C" represent averages of original unprocessed absorbances of three independent experiments (black, gray and white). Error bars represent standard deviations.

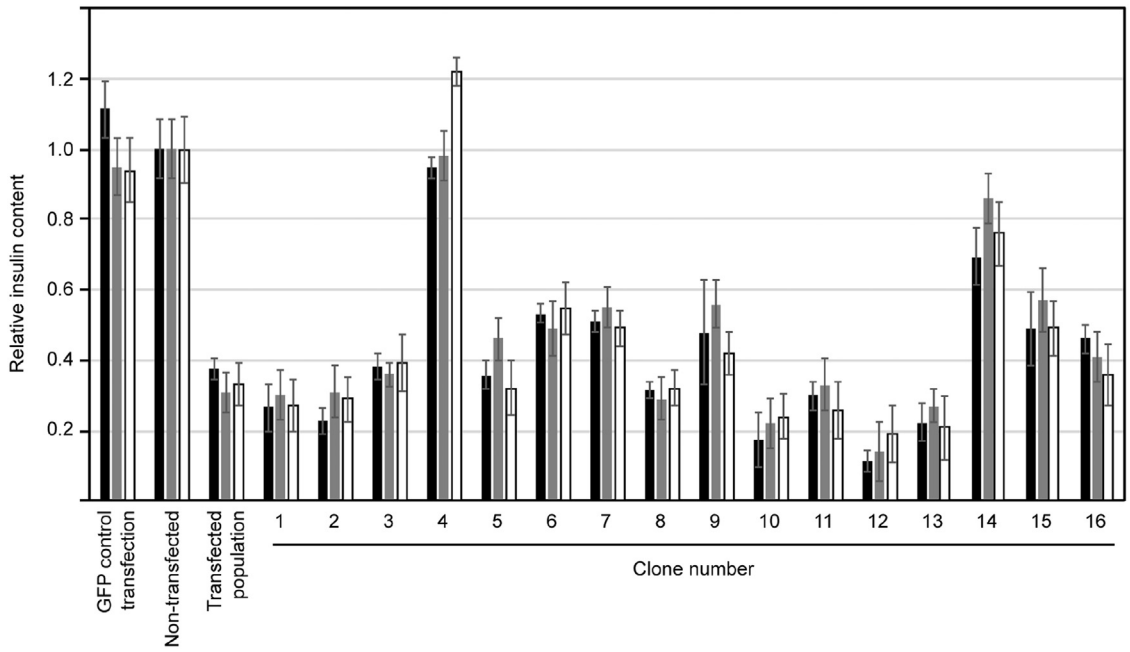

Fig. 4. Identification of INS-1 clones with reduced insulin content. Analysis of INS-1 clones reveals clones with reduced insulin content after normalizing to Janus Green B staining following exposure to lentiviral particles intended to permanently supply short hairpin iRNA targeting the transcription factor MafA for knockdown. Lines were analyzed serially three times each (represented by different gray bars) and compared to non-transfected controls. The transfected population as a whole and a GFP-control transfected population are also included for comparison. Bars represent averages of 4 wells normalized to control (non-transfected) and error bars represent standard deviations.

permeabilize the cells for the immunoreactivity reaction, when used without fixation resulted in free-floating nuclei intact with little cytoplasm allowing soluble insulin release for sandwich-ELISA analysis. Soluble insulin analysis was carried out in kit form (see Materials and Methods) as per manufacturer's recommendations except Triton X-100 was included in standard curves to maintain consistency between samples and standards. As expected, following 5-day exposure to high-glucose, insulin was reduced to similar levels as measured by either technique (Fig. 3B and C). Cell lysates had to be diluted (approximately 1% of each lysate was measured) to be within the linear range of the commercial sandwich-ELISA kit. Importantly, this demonstrated a higher sensitivity using lysate analysis compared to the cell-ELISA. The relative low immunoreactivity as measured by cell-ELISA may reflect the physiological granular structure of insulin within storage/secretory vessels, potentially restricting HRP-Ab from reaching the inner core of the structures. Nevertheless, cell-ELISA immunoreactivity paralleled total insulin content measurements (an approximate 50% decrease) as measured by either technique in response to hyperglycemia. The cell-ELISA technique however, has the advantage of processing multiple samples in unison efficiently in an economical fashion. In traditional ELISAs used for assessing insulin secretion into the culture supernatant, there is a potential of cell lysis, of which only of a few cells would cause an apparent burst release of insulin, potentially contributing to and over-estimating insulin measurements assumed to be of physiological origin. This specific monitoring of intracellular insulin described here is therefore a significant advantage because insulin immunoreactivity represents the culture condition at time of fixation without change in cell number after fixation (Supplemental Fig. 2).

2.4. Cell-ELISA identification of clones with reduced insulin content

One of our primary motives for developing the cell-ELISA assay is to routinely screen and compare cultures for variations in insulin content. To determine if this is possible we attempted to reduce insulin expression by downregulation of the transcription factor MafA. MafA is a transcription factor (of at least three master regulators, others being Pdx1 and NeuroD) thought to function in maintenance of the mature β-cell phenotype, most notably but not limited to insulin expression and processing [9–11]. INS-1 cells were subjected to commercial lentiviral particles designed to permanently integrate short-hairpin derived interference RNA specifically targeting MafA mRNA for inactivation. Following transfection the resulting population as a whole, a population of lentiviral-induced GFP-expressing cells, and various isolated clones (following puromycin selection and clone expansion over many weeks) were subjected to anti-insulin cell-ELISA and Janus Green B analysis, along with non-transfected cells as control cultures. Measurements were normalized to a standard curve derived by the application of different densities of non-transfected INS-1 cells applied to the identical assay plates the previous day. This allowed direct comparison of both insulin immunoreactivity and Janus Green B stain to a known number of cells, and because both are directly proportional to cell number (Supplemental Fig. 9), allowed normalization of relative insulin content. Initial cell counts for the standard curves were estimated using a hemocytometer, which we believe represents no more than $\pm 20\%$ accuracy. Trypan blue exclusion routinely indicates $>95\%$ viability following trypsinization of INS-1 cells. Typically, dilutions were used from an original cell suspension. This ensures that even if initial cell density is inaccurate, dilutions reflect relative cell numbers within the standard curve, within each experimental plate. This experimental approach allows analysis of 16 conditions (in this case 16 clones) and three control cultures (a non-transfected population, a transfected population and a GFP-transfected population), all compared with the standard curve on the identical plate, each in quadruplicate. A representative standard curve seeding from 5000 to 40,000 INS-1 cells and incubated overnight is displayed in Supplemental Fig. 9. A control lentiviral particle delivering green fluorescent protein was used as a transfection and puromycin exposure control, which was grown in parallel to MafA

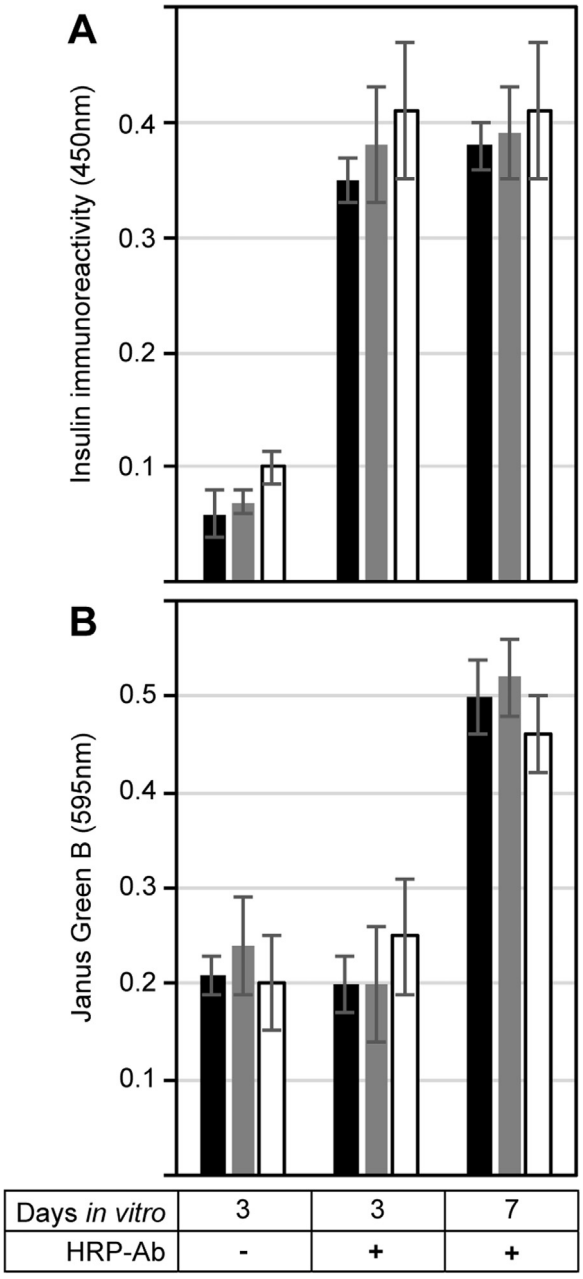

Fig. 5. Anti-insulin cell-ELISA on partially dissociated primary mouse islets. Partially dissociated mouse islets were seeded (approximately 20 islets per well) and analyzed after 3 and 7 days *in vitro*. For insulin immunoreactivity (A) and Janus Green B (B), bars represent averages of original unprocessed absorbances of four wells from three independent experiments (black, gray and white). Error bars represent standard deviations.

mRNA targeted cultures. The standard curve ultimately inferred relative insulin between cultures (between clones and between controls) normalized to cell density. Identical clones were twice more analyzed in series which confirmed insulin reduction in identical clones, and demonstrated the cell-ELISA technique is reliable (Fig. 4). Further application of a fluorescently labeled anti-mouse antibody to identify the presence of the initial HRP-conjugated anti-insulin antibody on the identical assay plates confirmed reduced anti-insulin fluorescence (visually) which paralleled cell-ELISA immunoreactivity reduction (Supplemental Fig. 10). The clones are not fully characterized at this time and levels of potentially compensatory transcription factors other than MafA have not been investigated. We are not attempting here to propose the specific mechanism of insulin reduction nor speculate on possible cellular adaptations. The purpose of this experiment was to demonstrate that this technique is successfully able to efficiently screen multiple cultures for variations in insulin protein content.

2.5. Utilization of anti-insulin cell-ELISA on primary islet-cell cultures

Our ultimate goal is to apply this method to monitor insulin content within primary islet cell cultures. To demonstrate the feasibility of this assay on primary tissues, partially dissociated mouse islets were utilized. Mouse pancreas tissue was digested with collagenase and islets were isolated by handpicking, partially dissociated with trypsin and seeded into 96-well plates previously coated with fibronectin. Approximately 20 partially dissociated islets of random sizes were seeded per well and analyzed after 3 and 7 days. Cell-ELISA analysis indicated that insulin immunoreactivity was present and relatively unchanging over this time (Fig. 5A). The Janus Green B assay, as expected, demonstrated an increase in cell density over this culture period due to proliferation of non-β-cells (Fig. 5B). It should be noted, however, that the mechanism of Janus Green B staining of fixed cells has not been established, and may therefore be a source of error within primary culture density analysis. Non-α and non-β proliferating cells routinely contaminate our islet cell cultures and likely lead to the observed increase in Janus Green B staining. In our hands (in experiments not described here) we have yet to observe insulin-positive (nor glucagon-positive) cells simultaneously positive for the proliferation marker Ki-67, suggesting our β-cells are not proliferating but surviving over this culture period as other cell types continue to proliferate.

3. Conclusions

We were successful in optimizing and validating the cell-ELISA method to monitor relative intracellular insulin content in culture. Importantly, this method relies on soluble colored products which are measured by absorbance of in-place liquids. This is an advantage over direct visual observations of immunocytochemistry by eliminating preconception and bias as fields of view can change dramatically, particularly in primary cultures such as partially dissociated mouse islets which exhibit from few to many insulin-positive cells per field of view.

The cell-ELISA technique measures relative intracellular insulin which is distinct from secreted insulin measurements. The technique is not expected to replace extracellular insulin analysis. As secreted insulin within a medium corresponds to an accumulation over time (secreted and lysed), it is not expected to match the intracellular insulin remaining after cell lysis, secretion, and/or degradation due to intracellular insulin being replaced within viable β-cells continuously. Much of the kinetics of insulin biochemistry (such as turnover time following secretion and intracellular degradation) are not properly characterized in the published literature. This assay may aid in these investigations. However, this also imposes a limitation on the assay because it does not take into account physiological activity of β-cells; expression does not imply a physiological response to glucose stimulation as demonstrated in the literature [12]. Prior to fixation, supernatants can be stored for further secreted insulin measurements if and when required. This technique therefore reduces the reliance on secreted insulin analyses, with caution that it corresponds to analysis of a single time point.

Additionally, it is not unexpected that culture conditions will alter insulin expression or content. However, because analyses are

performed on a single plate, culture-to-culture variances are expected to be minimized. This is evident upon the observation of high R^2-values in each of the figures presented. It should be noted there are also variances between cells within each well. For example, occasional highly expressing cells can be found within an insulin-reduced clone population, as noted in Supplemental Fig. 10. Insulin immunoreactivity values are directionally proportional to cell density, but thousand of cells are required for confident results. Results reflect immunoreactivity on a per cell basis, but obtained over the means of a substantial number of cells. With this cell-ELISA assay, a few highly insulin-expressing cells therefore do not generate false-positive reactions as opposed to assays measuring released soluble insulin. In fact, burst-released insulin, from damaged or death cells, can result in an overestimation of assumed physiologically secreted insulin.

A potential limitation of this technique is the probable restriction of the HRP-Ab to only recognize insulin molecules at the periphery of the normally granular-like insulin structures within secretory/storage vesicles. This assay must therefore rely on the assumption that insulin structures are, over an average, of uniform size and density. However, because the described correlations between cell density and insulin immunoreactivity from either cell-ELISA or cell lysates are equivalent, and due to the observed high R^2 values, this assumption is reasonable. From our understanding, the dynamics of insulin vesicle formation and morphology have not been adequately addressed in the literature to answer these questions.

To apply the technique to biological questions, we screened and identified several INS-1 clones with reduced insulin content by means of cell-ELISA with confirmation using immunocytochemistry. Finally, it was demonstrated that this method is applicable to mouse islets, revealing that insulin content remains relatively stable from 3 to 7 days *in vitro*. This technique, by providing an initial screen for further culture analysis on selected samples, essentially reduces the necessity to monitor insulin release or cell lysates as the primary screen.

The cell-ELISA technique utilizes equipment common to most cell biology laboratories. In our hands the cost of the required materials combining the cell-ELISA, Janus Green B and immunocytochemistry procedures for a single 96-well plate is approximately 1/25th that of a typical 96-well plate commercially used to determine soluble (secreted) insulin and cell lysates content (Supplemental Table).

We anticipate this method to be applicable for many explorations including 1) optimizing β-cell differentiation/proliferation/culture conditions; 2) insulin biochemistry; and 3) medium throughput screening (including simultaneous combinations). Although cell-ELISA has limitations, it provides the first opportunity to routinely, efficiently and economically monitor intracellular insulin levels intended as an initial screen for investigating fundamental β-cell biology questions.

4. Materials and methods

4.1. General cell line maintenance

The rat β-like cell line INS-1 was obtained from AddexBio (San Diego, California, USA, C0018007) and the human pancreatic ductal cell line PANC-1 was obtained from ATCC (USA, Manassas, Virginia, CRL-1469). INS-1 and PANC-1 cells are routinely cultured in RPMI medium (Sigma-Aldrich, R1383) or DMEM medium (Sigma-Aldrich, D5523) respectively, containing 5.6 mM glucose (without pyruvate) and 1.7 g/L $NaHCO_3$, pH corrected to approximately 7.2, plus 10% fetal bovine serum (Thermo Fisher Scientific, Gibco 12483-020). INS-1 cell culture medium was supplemented with 50 μM β-mercaptoethanol (Sigma-Aldrich, M3148). Cultures were grown at 37 °C in a humidified 5% CO_2 atmosphere. Cultures were routinely fed 3 times a week with β-mercaptoethanol and serum being supplied fresh weekly, and passaged using 0.25% trypsin-EDTA (Thermo Fisher Scientific, Gibco 25200-056) for 2–3 min at 37 °C before confluence. During experiments in 96-well plates, cultures were routinely fed every 2 days by replacing 50% of the culture medium with fresh medium. Except where noted, glucose was kept constant at 5.6 mM.

4.2. Experimental scheme

For experimental analysis, 96-well plates were prepared by exposing overnight to 0.05 mg/mL poly-L-Lysine (30,000–70,000 MW, Sigma-Aldrich, P9155) before adding cells to ensure near 100% plating efficiency. Log-phase cells were trypsinized, diluted with growth medium and centrifuged at 1k rpm (the minimal setting for this laboratory) for 3 min to remove debris. Viability, estimated by trypan blue exclusion, was routinely $>95\%$. Cell densities were determined with a hemocytometer and cells diluted to seed at various densities depending upon expected time in culture before analysis. Cell standard curves were applied the day before analysis. The final culture volume was kept consistent at 150 μL/well.

Cell-ELISA, Janus Green B staining and fluorescent imaging were performed sequentially on identical wells. Immediately prior to fixation, culture plates were rotated on a titer plate shaker (Thermo Fisher Scientific, Lab-Line Instruments Inc.) for 8 s on setting #7 to loosen cell debris. Directly to the existing culture medium an equal volume of 4% freshly-depolymerized formaldehyde in Dulbecco's phosphate buffered saline (PBS) with calcium and magnesium (Thermo Fisher Scientific, Gibco 14080-055) was added to each well and left at room temperature. After 20 min, plates were placed on the titer plate shaker for an additional 10 min to give a total fixation time of 30 min. All further steps were performed at room temperature on the shaker at setting #7 except when the plates were stored at 4 °C overnight (see below). Plates were washed 7 times over 30 min (5 min between washes) with PBS (Fisher Bioreagents, BP665-1) containing 0.25 mL/L Tween-20 (PBST) with the inclusion of 0.5% Triton X-100 in the third wash (5 min) to permeabilize cell membranes (200 μL/well/wash). When analyzing primary tissue, the fifth wash included 1% H_2O_2 to quench possible endogenous peroxidase activity. Blocking solution (5% Carnation fat-free instant skim milk powder in PBST) was applied for 60 min (300 μL/well). Horseradish peroxidase-conjugated anti-insulin (Abcam, ab28063) was diluted (1:2000) in blocking solution and applied for 60 min (50 μL/well). Plates were washed 7 times over 30 min with PBST and "Slowest Kinetic Rate" TMB ELISA substrate (Abcam, ab171527) was added (100 μL/well). After 5 min, 1 M HCl in 140 mM NaCl was added (100 μL/well) and absorbance read at 450 nm. All absorbance readings were made with a Synergy HT plate reader with Gen 5 software (both from Bio-Tek industrial, Winooski, Vermont, USA). Plates were washed 7 times over 30 min with PBST and stained with 0.3% Janus Green B (Sigma-Aldrich, 201677) in PBS or Janus Green B cell normalization stain (Abcam, ab111622) for 5 min (50 μL/well). Plates were washed 7 times over 30 min with PBST then rinsed once more quickly with 140 mM NaCl (non-buffered) and exposed to 0.5 M HCl in 140 mM NaCl (100 μL/well). After 10 min, absorbances were read at 595 nm. Plates were washed 7 times over 30 min with PBST. Alexa 488-conjugated goat anti-mouse (1:2000, Life Technologies, A11001) plus Hoechst 33258 (2 μg/mL) and 0.01% thimerosal (as a preservative; Sigma-Aldrich, T8784) in blocking solution was applied overnight at 4 °C without shaking (50 μL/well). Next morning, plates were brought to room temperature and washed 7 times over 30 min with PBST

before image acquisition.

4.3. Experimental manipulations

To osmotically lyse cells, medium was replaced with distilled water and culture plates returned to the culture incubator for 5 min. Following the initial titer plate shake (see above), all cells were lysed and eventually washed away as the procedure progressed. To pre-adsorb the HRP-Ab antibody, 200-fold excess (w/w) of bovine insulin (Sigma-Aldrich, I0516) was combined with working strength antibody in blocking solution for 1 h during the blocking reaction (see above), and then applied in place of the native HRP-Ab. To apply the capture anti-insulin antibody, the capture antibody (Abcam, ab8304) was diluted in 100 mM carbonate-bicarbonate buffer (pH 9.6, 50 μL/well) and applied overnight to wells on the assay plate previously intentionally left without culture medium. Wells were rinsed twice with PBS and bovine insulin in culture medium was applied (spiked) into these wells and negative control sister wells void of the capture antibody for 1 h prior to fixation. To measure total insulin content using a commercial sandwich-ELISA kit (ALPCO rat high range ELISA 80-INSRTH-E01, Salem, New Hampshire, USA), cultures were rinsed with PBS and exposed to 0.5% Triton X-100 in PBST (the identical Triton X-100 concentration used in the permeabilization step above) for 5 min at room temperature. Samples were then triturated with a 200 μL pipette tip, which left floating nuclei intact without significant cell debris. Samples were centrifuged for 1 min (14,000 rpm) to sediment nuclei, and supernatants were stored frozen for later insulin content analysis as per manufacturer's instructions.

4.4. Primary islet cultures

Animals were used in accordance with the local University ethical committee and animal guidelines (protocol #367-14). Female adult CD-1 mice, approximately 20 g, were euthanized by CO_2 asphyxiation and the pancreas was removed and immediately infused with 1 mg/mL collagenase (type V from Clostridium histolyticum; Sigma-Aldrich, C9263) in L15 nutrient mix (Sigma-Aldrich, L4386) supplemented with 5.6 mM glucose, 10 mM nicotinamide, 15 mM HEPES, 50 μM β-mercaptoethanol and 10% FBS on ice for transport. The pancreatic tissue was dissociated for approximately 15–20 min with occasional brisk inversion. Under a dissecting microscope, islets were hand-picked and placed in culture medium consisting of DMEM and RPMI at a 1:1 ratio, supplemented with 10% FBS, 50 μM β-mercaptoethanol, 10 mM nicotinamide and 25 mM N-acetyl-L-cysteine, 15 mM HEPES, 1.7 g/L $NaHCO_3$ and 5.6 mM glucose. Tissues pieces which were not initially digested were placed back into fresh dissociation medium and digested for another 5–10 min until islets were released. Islets were pooled and counted. Samples were tested for viability using a live/dead viability kit for mammalian cells (Thermo Scientific, L3224) as per manufacturers' instructions. Islets preparations estimated to be $>90\%$ viable were used. Islets were rinsed with Hank's balanced salt solution (HBSS) (by gravity sedimentation) and incubated with 0.125% trypsin plus ethylene diamine tetraacetic acid on ice for 30 min then placed at 37 °C for 5–8 min. The tissue was returned into culture medium with one rinse (by gravity sedimentation) and seeded into 96-well culture plates at approximately 20 dissociated islets per well. Culture plates were pre-exposed (on the day of tissue application) to 2 μg/cm^2 fibronectin (EMD Milipore, Darmstadt, Germany, FC010). Cultures were incubated at 37 °C in a 5% CO_2 humidified atmosphere.

4.5. Lentiviral particle exposure and cloning

INS-1 cells were seeded at a density of 20,000 cells per well into two single wells of a 96-well plate one day prior to transfection. Medium was replaced with fresh medium supplemented with 5 μg/mL polybrene® (Santa Cruz Biotechnology, sc-134220), 100 μL per well. The lentiviral particles, MafA shRNA (h) (Santa Cruz, sc-43905-v) and control copGFP (Santa Cruz, sc-108083), were added separately to each well, 20 μL and 10 μL, respectively. As per the manufacturer's confirmation, the shMafA lentiviral contains a short-hairpin construct producing the sense strand: 5′-GGACCUGUACAAGGAGAAA-3′ specifically targeting to knock down both rat and human MafA mRNA. After two days, the cultures were passaged by trypsinization for propagation in the presence of puromycin dihydrochloride (Santa Cruz, sc-108071) added at a final concentration of 1 μg/mL as a selection reagent. For cloning, less than 100 cells were visually inspected to confirm a complete single cell suspension, diluted into 160 mL growth medium (with puromycin) and seeded into eight 96-well plates. After one week, 50% of the medium was exchanged for fresh medium with puromycin decreased to 0.25 μg/mL. After two weeks, wells with a single colony were identified and assumed to be a single clone. These wells were fed weekly by replacing 50% of the medium with fresh, containing 0.25 μg/mL puromycin. All further feedings contained 0.25 μg/mL puromycin. Screening was initiated when clones were of sufficient numbers for continued propagation (approximately 5–6 weeks following initial transfection). Clones (and full populations of transfected cells) were passaged into dishes for further propagation and 96-well plates for insulin screening. When wells were approximately 50% confluent, a standard curve consisting of non-transfected INS-1 cells was incorporated onto the same assay plates at densities ranging from 5000 to 40,000 cells per well. Insulin and Janus Green B analysis of clones, transfected populations and standard curves were done in quadruplicate on each plate. Cultures were assayed the day after application of INS-1 cells as the standard curve.

4.6. Photo microscopy

For bright field and phase contrast imaging, wells were filled with culture medium, water or PBST (to match the solute in place) and covered with a glass slide to eliminate the meniscus such that Köhler illumination and phase contrast rings could be properly adjusted (Supplemental Fig. 1). Cells were observed with a Nikon inverted microscope (Nikon Eclipse TE2000-S) and images taken using a Zeiss AxioCam MRm camera with Zeiss AxioVision SE64 software. Alexa-488 images within each figure were taken at identical exposures and when color was applied, was added using Photoshop CS5.

4.7. Data analysis

Determination of means, standard deviations, p-values and R^2 values were calculated with Excel software.

Author contributions

PLA devised and performed the experiments, analyzed the data, and wrote the initial manuscript. PV reviewed and edited the manuscript. PLA and PV reciprocally re-edited until mutual agreement on the final document.

Acknowledgments

This work was supported by the Quebec Consortium for Drug Discovery (CQDM) awarded to PV. The authors acknowledge the Vermette's laboratory members for helpful thoughts and the all-important critical arguments. PLA is also grateful to Dr. David J Schreyer for initial mentoring with the cell-ELISA technique.

Appendix A. Supplementary material

Supplementary data associated with this article can be found in the online version at http://dx.doi.org/10.1016/j.yexcr.2016.06.014.

Supplementary items are attached below references.

References

[1] F.W. Pagliuca, D.A. Melton, How to make a functional beta-cell, Development 140 (2013) 2472–2483.
[2] R. Falahat, M. Wiranowska, N.D. Gallant, R. Toomey, R. Hill, N. Alcantar, A cell ELISA for the quantification of MUC1 mucin (CD227) expressed by cancer cells of epithelial and neuroectodermal origin, Cell Immunol. 298 (2015) 96–103.
[3] D.J. Schreyer, P.L. Andersen, K. Williams, I. Kosatka, T.N. Truong, Quantitative analysis of GAP-43 expression by neurons in microcultures using cell-ELISA, J. Neurosci. Methods 72 (1997) 137–145.
[4] M. Asfari, D. Janjic, P. Meda, G. Li, P.A. Halban, C.B. Wollheim, Establishment of 2-mercaptoethanol-dependent differentiated insulin-secreting cell lines, Endocrinology 130 (1992) 167–178.
[5] G. Raspotnig, G. Fauler, A. Jantscher, W. Windischhofer, K. Schachl, H.J. Leis, Colorimetric determination of cell numbers by Janus green staining, Anal. Biochem. 275 (1999) 74–83.
[6] Y.M. Leung, L. Sheu, E. Kwan, G. Wang, R. Tsushima, H. Gaisano, Visualization of sequential exocytosis in rat pancreatic islet beta cells, Biochem. Biophys. Res. Commun. 292 (2002) 980–986.
[7] S.S. Andrali, M.L. Sampley, N.L. Vanderford, S. Ozcan, Glucose regulation of insulin gene expression in pancreatic beta-cells, Biochem. J. 415 (2008) 1–10.
[8] L.K. Olson, J. Qian, V. Poitout, Glucose rapidly and reversibly decreases INS-1 cell insulin gene transcription via decrements in STF-1 and C1 activator transcription factor activity, Mol. Endocrinol. 12 (1998) 207–219.
[9] H. Kaneto, T.A. Matsuoka, S. Kawashima, K. Yamamoto, K. Kato, T. Miyatsuka, N. Katakami, M. Matsuhisa, Role of MafA in pancreatic beta-cells, Adv. Drug Deliv. Rev. 61 (2009) 489–496.
[10] Y. Hang, R. Stein, MafA and MafB activity in pancreatic beta cells, Trends Endocrinol. Metab. 22 (2011) 364–373.
[11] Y. Hang, T. Yamamoto, R.K. Benninger, M. Brissova, M. Guo, W. Bush, D. W. Piston, A.C. Powers, M. Magnuson, D.C. Thurmond, R. Stein, The MafA transcription factor becomes essential to islet beta-cells soon after birth, Diabetes 63 (2014) 1994–2005.
[12] K.A. D'Amour, A.G. Bang, S. Eliazer, O.G. Kelly, A.D. Agulnick, N.G. Smart, M. A. Moorman, E. Kroon, M.K. Carpenter, E.E. Baetge, Production of pancreatic hormone-expressing endocrine cells from human embryonic stem cells, Nat. Biotechnol. 24 (2006) 1392–1401.

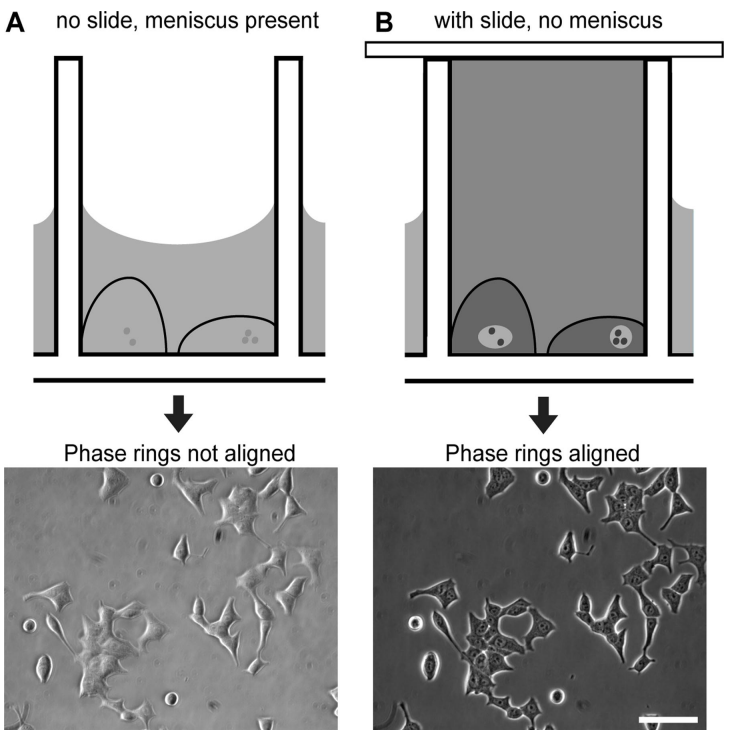

Supplemental Figure 1 - Removal of meniscus to reveal cell morphology. The curvature of the meniscus inhibits phase contrast imaging (**A**). Filling the well with appropriate fluid and covering with a glass slide allows Köhler illumination and phase contrast microscopy (**B**). Bar = 50 µm.

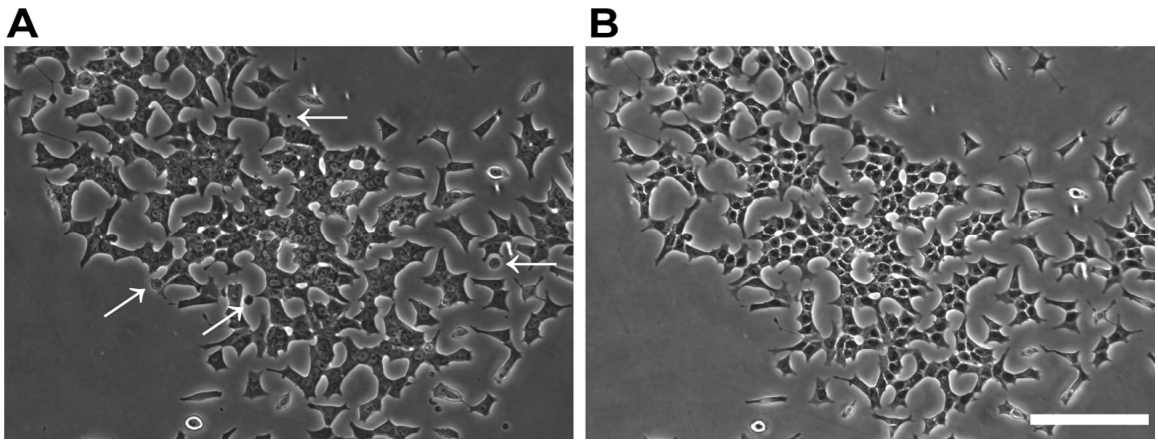

Supplemental Figure 2 - Appearance of INS-1 cell cultures. Phase contrast images of near identical fields of view were taken before fixation (**A**) and following the entire protocol (cell-ELISA, Janus Green B stain release and immunocytochemistry, **B**). Although morphology has changed, cell number and position remain virtually consistent. Some debris (arrows in "**A**" as examples) have been detached. Bar = 50 μm.

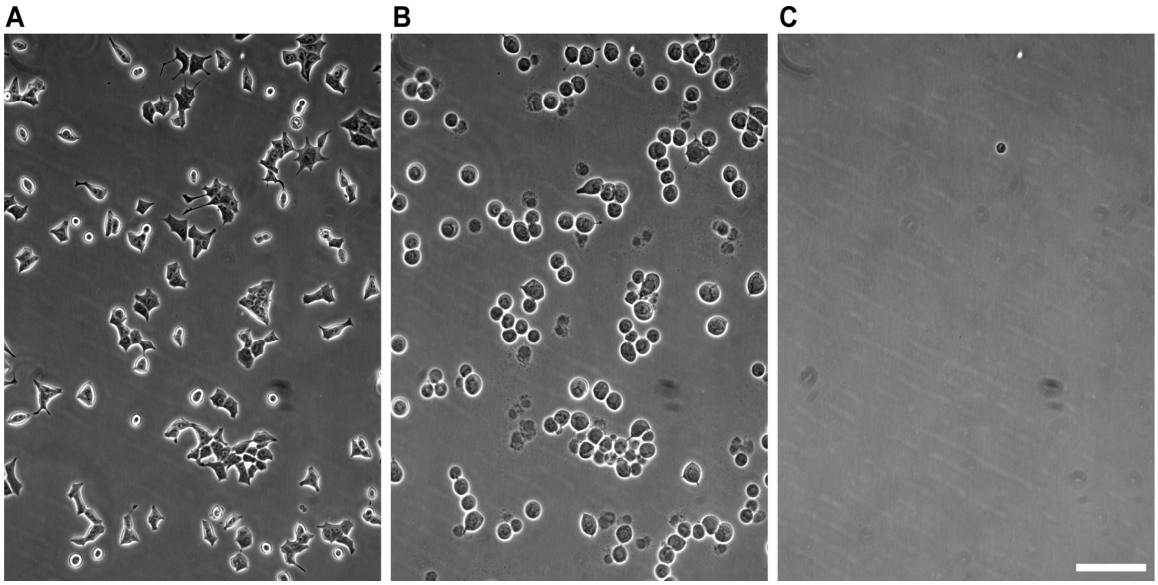

Supplemental Figure 3 – Osmotically-lysed INS-1 cells are removed from cell-ELISA analysis. Phase contrast images of near-identical fields of view were captured before (**A**), during (**B**) and following osmotic lysis and agitation (**C**) by replacing culture medium with water. Scale bar = 50 µm.

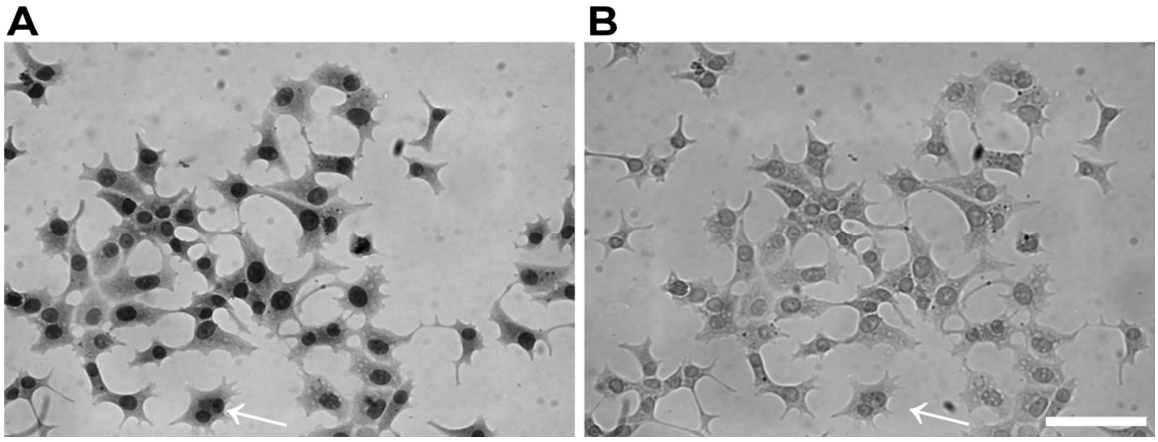

Supplemental Figure 4 - Janus Green B staining of INS-1 cells. Bright field near identical fields of view were photographed following staining before (**A**) and after (**B**) acid release. Note binucleate cells were occasionally present (arrows in "**A**" and "**B**"). Bar = 50 µm.

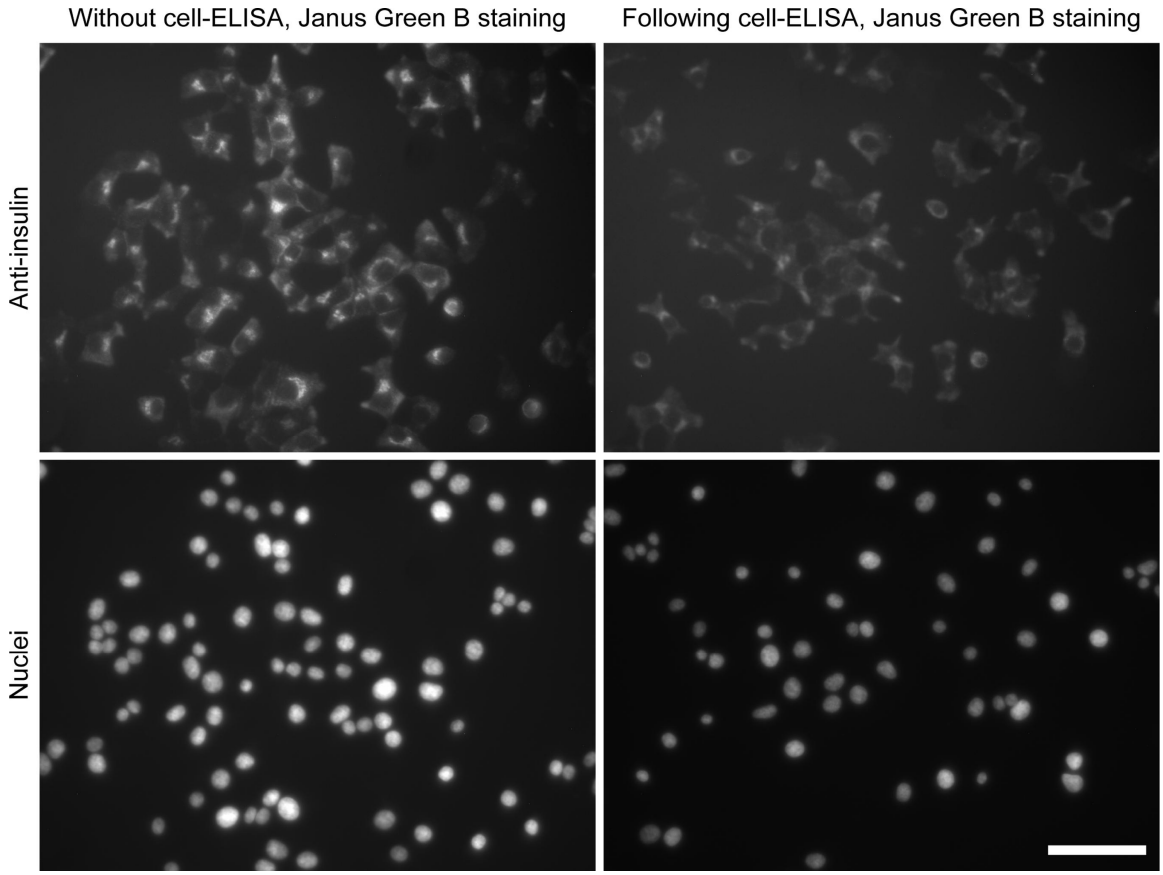

Supplemental Figure 5 - The effects of cell-ELISA and Janus Green B staining on anti-insulin immunofluorescence. Anti-insulin immunofluorescent images (**upper panel**) were captured without (**left column**) or following cell-ELISA and Janus Green B staining (**right column**). Nuclei of corresponding fields of view are revealed by Hoechst 33258 staining (**lower panel**). Bar = 50 µm.

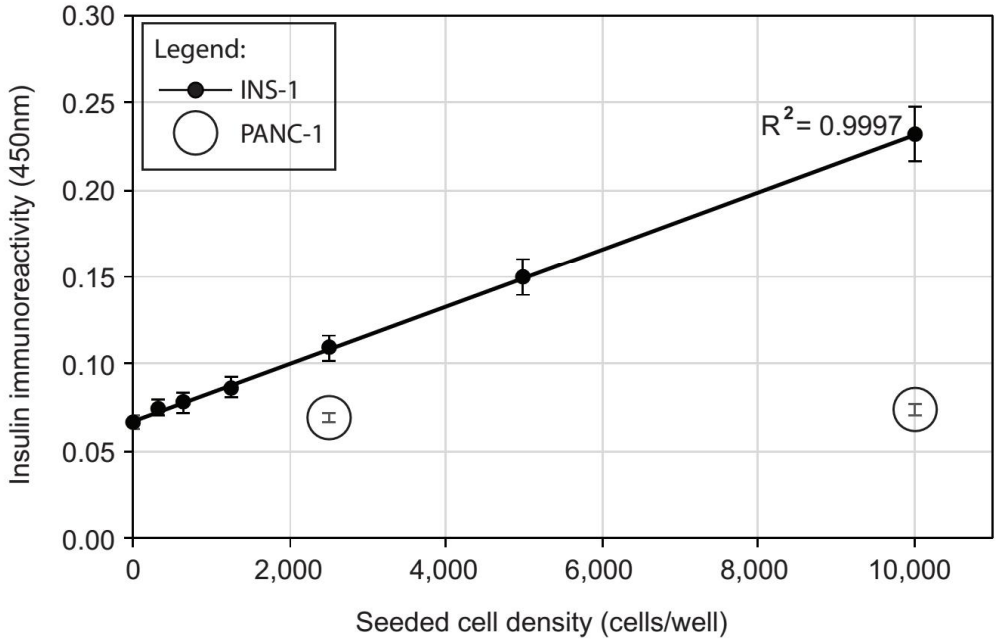

Comparing seeded cell densities: ↓ vs. →		PANC-1		INS-1					
		2,500	10,000	312	625	1,250	2,500	5,000	10,000
INS-1	0	0.1917545	0.0017821	0.0024659	0.001102	9.449E-06	4.305E-08	5.563E-09	3.454E-09
	10,000	9.079E-09	7.172E-09	2.932E-09	1.029E-09	1.346E-09	2.453E-09	3.888E-08	
	5,000	3.426E-08	2.386E-08	5.746E-09	1.965E-09	6.728E-09	6.445E-07		
	2,500	3.899E-07	4.634E-07	2.034E-07	4.709E-07	2.152E-05			
	1,250	5.053E-05	0.0004468	0.0010363	0.0135694				
	625	0.0044268	0.1330449	0.2914128					
	312	0.0108661	0.6294918						
PANC-1	10,000	0.0057784							

Supplemental Figure 6 - Analysis of insulin immunoreactivity sensitivity based on statistical p-values. INS-1 cells were diluted two-fold in series and processed for insulin immunoreactivity (cell-ELISA). The table lists statistical p-values between data points on the corresponding plot. The same plate was further processed for cell density analysis (Janus Green B staining, **Supplemental Figure 7**). Data points represent averages of eight wells +/- standard deviations. The solid line with black circles corresponds to INS-1 cell cultures. Clear circles, expanded to reveal error bars, correspond to PANC-1 cell cultures. The R^2 value is included to demonstrate linearity.

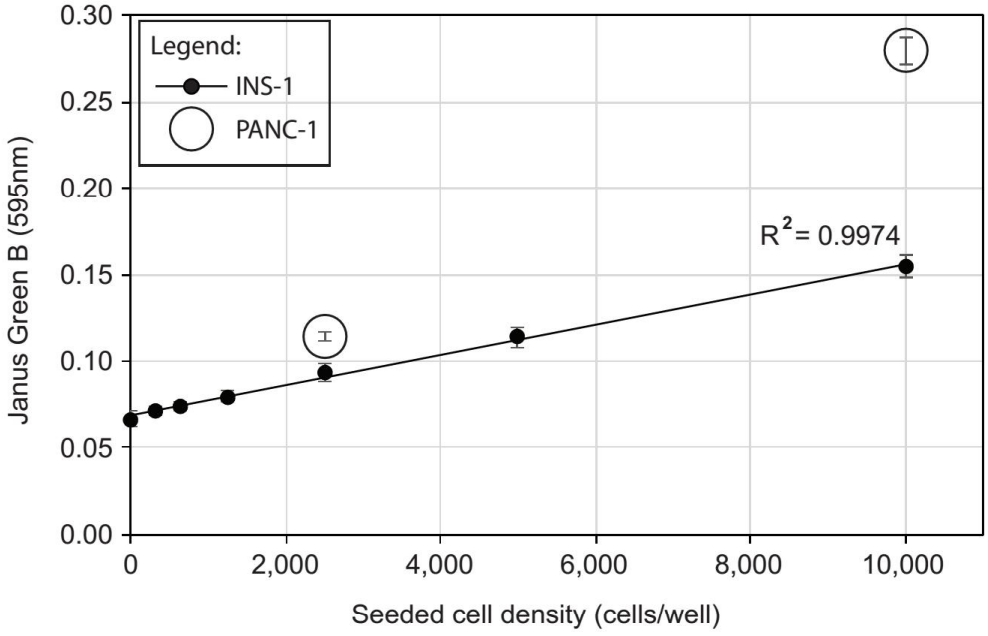

Comparing seeded cell densities: ↓ vs. →		PANC-1		INS-1					
		2,500	10,000	312	625	1,250	2,500	5,000	10,000
	0	5.492E-12	2.752E-15	0.0298349	0.0012036	4.851E-06	5.711E-08	1.109E-09	2.111E-13
INS-1	10,000	2.964E-08	1.141E-14	1.244E-11	5.039E-12	1.125E-11	5.308E-12	3.215E-09	
	5,000	0.8020515	1.919E-16	2.018E-08	2.105E-08	9.72E-08	9.471E-06		
	2,500	2.414E-06	1.631E-16	8.474E-07	2.581E-06	7.154E-05			
	1,250	2.548E-12	8.021E-14	2.964E-05	0.0023938				
	625	3.94E-13	5.945E-14	0.0503821					
	312	1.1E-14	1.969E-13						
PANC-1	10,000	4.732E-12							

Supplemental Figure 7 - Analysis of Janus Green B staining sensitivity based on statistical p-values. INS-1 cells were diluted two-fold in series and previously processed for insulin cell-ELISA (**Supplemental Figure 6**), then processed to determine cell densities using Janus Green B staining. The table lists statistical p-values between data points on the corresponding plot. Data points represent averages of eight wells +/- standard deviations. The solid line with black circles corresponds to INS-1 cell cultures. Clear circles, expanded to reveal error bars, correspond to PANC-1 cell cultures. The R^2 value is included to demonstrate linearity.

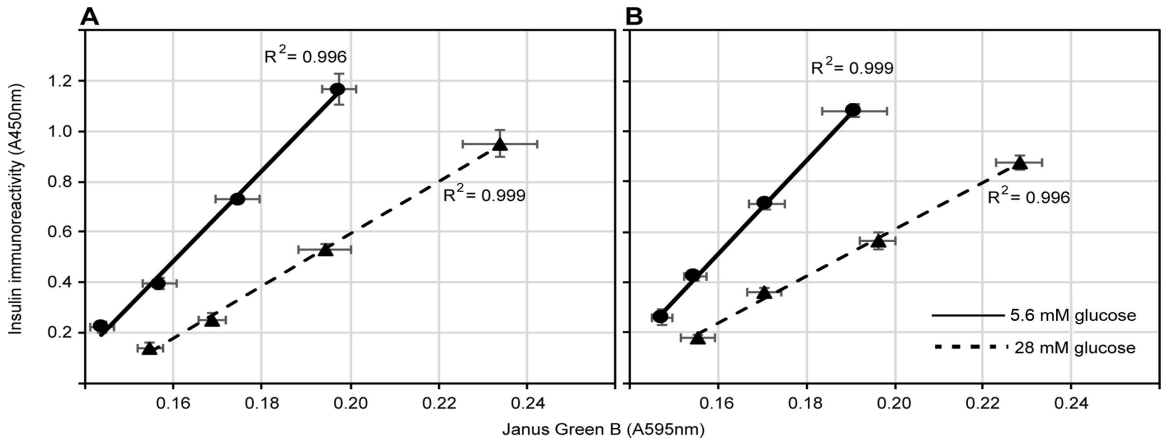

Supplemental Figure 8 - Re-validation of the cell-ELISA assay. To repeat data presented in Figure 3, insulin immunoreactivity (A450nm) and Janus Green B release (A595nm) were twice more (**A** and **B**) determined after five-day exposure to 5.6mM (solid line) or 28mM (dashed line) glucose. Cells were initiated at various densities identically between the two glucose conditions. Each point represents an average of six (**A**) or eight wells (**B**). Error bars represent standard deviations within each representative experiment, and R^2 values are included to demonstrate linearity.

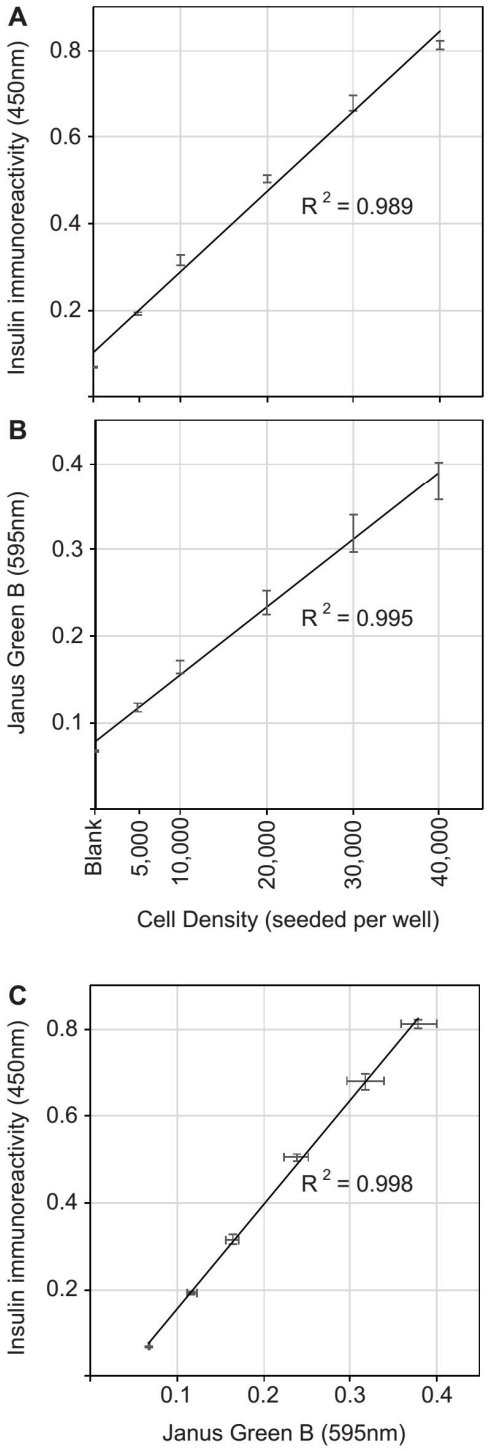

Supplemental Figure 9 - INS-1-derived standard curves. INS-1 cells were seeded without (blank) and with cells ranging from 5,000 to 40,000 cells per well in quadruplicate, on each assay plate. The next day, plates were assayed for insulin immunoreactivity (**A**) or Janus Green B staining (**B**). This gives a direct relation between cell number and relative insulin content with the correlation shown on the graph (**C**). Bars indicate the standard deviations between four wells. Data points (means of four wells) are not included to reveal error bars. The R^2 values are included to demonstrate linearity.

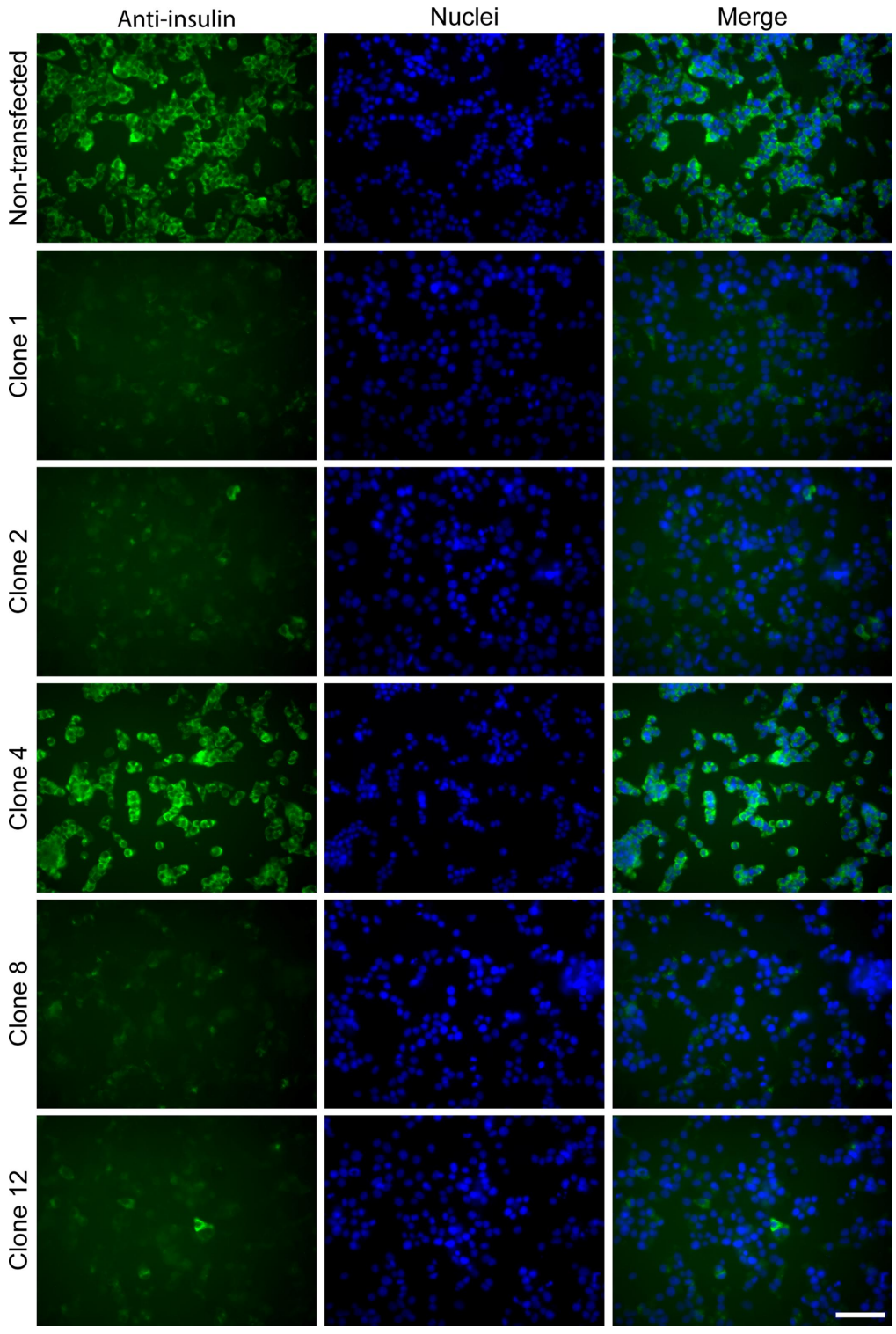

Supplemental Figure 10 - Anti-insulin immunocytochemistry of selected INS-1 clones. Directly from the assay plate (corresponding to Fig. 4A, black bars), selected clones were photographed for immunofluorescence to compare with relative measured insulin levels (**Figure 4**). Green indicates insulin immunoreactivity (**left panel**), with counterstain Hoechst 33258 to identify nuclei (**center panel**). The merge of the two staining (**right panel**) of the clone numbers and a non-transfected control population is also shown. Bar = 50 µm.

Supplemental Table: Cost comparison between cell-ELISA and commercial soluble-ELISA kits.

Component	Unit cost (CAD)	Unit	Capacity (plates)	Cost/plate (CAD)	Average cost per plate (CAD)
TMB solution	49	100 mL	10	4.90	16
Janus Green B	72.40	5 g	>200	< 0.50	
488-anti-mouse	223.65	500 µL	200	1.12	
HRP anti-insulin	383	200 µg	40	9.56	
Rat high-range anti-insulin ELISA	6194	1	16 (bulk)	387	387-482
	482	1	1	482	

All prices are derived from the internet before shipping, handling and taxes in Canadian currency as of December 2015. These items are of common use in Vermette's laboratory. Buffers, plastics and other common laboratory reagents are excluded. One "plate" refers to 96 wells.